Nanoscale Research Letters

RESEARCH Open Access

Gold Nanoparticles Enhancing Generation of ROS for Cs-137 Radiotherapy

Shiao-Wen Tsai[1,2], Chang-Yun Lo[3], Shang-Yang Yu[3], Fang-Hsin Chen[4,5,6], Hsiao-Chieh Huang[5,7], Lu-Kai Wang[8] and Jiunn-Woei Liaw[3,7,9*]

Abstract

Radiotherapy is an important modality for the treatment of cancer, e.g., X-ray, Cs-137 γ-ray (peak energy: 662 keV). An important therapy pathway of radiation is to generate the double strand breaks of DNA to prohibit the proliferation of cancer cells. In addition, the excessive amount of reactive oxygen species (ROS) is induced to damage the organelles, which can cause cellular apoptosis or necrosis. Gold nanoparticles (GNPs) have been proven potential as a radiosensitizer due to the high biocompatibility, the low cytotoxicity and the high-*Z* property ($Z=79$) of gold. The latter property may allow GNPs to induce more secondary electrons for generating ROS in cells as irradiated by high-energy photons. In this paper, the radiobiological effects on A431 cells with uptake of 55-nm GNPs were studied to investigate the GNPs-enhanced production of ROS on these cells as irradiated by Cs-137 γ-ray. The fluorescence-labeling image of laser scanning confocal microscopy (LSCM) shows the excessive expression of ROS in these GNPs-uptake cells after irradiation. And then, the follow-up disruption of cytoskeletons and dysfunction of mitochondria caused by the induced ROS are observed. From the curves of cell survival fraction versus the radiation dose, the radiosensitization enhancement factor of GNPs is 1.29 at a survival fraction of 30%. This demonstrates that the tumoricidal efficacy of Cs-137 radiation can be significantly raised by GNPs. Because of facilitating the production of excessive ROS to damage tumor cells, GNPs are proven to be a prospective radiosensitizer for radiotherapy, particularly for the treatment of certain radioresistant tumor cells. Through this pathway, the tumoricidal efficacy of radiotherapy can be raised.

Keywords: Cs-137, Radiotherapy, Gold nanoparticles, Reactive oxygen species, Radiosensitizer, Disruption of cytoskeleton, Mitochondrial damage, Amplification factor, Radiosensitization enhancement factor, Tumoricidal efficacy

Introduction

Radiotherapy utilizing high-energy photon (e.g., X-rays and Cs-137 γ-ray) beam or proton beam is a useful modality for cancer treatment. Two mechanisms of radiotherapy causing the apoptosis or even necrosis of tumor cells were extensively studied; the double strand break (DSB) of DNA in cells by ionization, and the damage on cellular organelles by the produced reactive oxygen species (ROS), e.g., hydroxyl free radicals [1–4]. Recently, a variety of radiosensitizers to enhance the efficacy of radiotherapy has been developed [5–7]. In particular, using gold nanoparticles (GNPs) to produce excessive ROS for raising the tumoricidal efficacy of radiation therapy has attracted a lot of attentions [8–15]. Since gold is a high Z material ($Z=79$) with good biocompatibility and low cytotoxicity, GNP is a prospective candidate as radiosensitizer [12–16]. Various GNPs with different shapes, sizes and coatings (surface modifications) were developed to increase the cellular uptake and used as radiosensitizer for X-rays, Gamma ray of Cs-137 and even proton therapy

*Correspondence: markliaw@mail.cgu.edu.tw

[3] Department of Mechanical Engineering, Chang Gung University, Taoyuan, Taiwan
Full list of author information is available at the end of the article

[17–24]. A few of papers have shown that ultrasmall GNPs (e.g., 2–6 nm) can pass through nuclear pore into nucleus, whereas larger GNPs (size > 10 nm) only stay in cytoplasm [21]. In addition, several previous research works demonstrated that bare and spherical GNPs with an average diameter of 50 to 55 nm are more easily internalized by cells with low cytotoxicity [22, 25–27]. Recently, Chithrani et al. found that 50-nm GNPs perform the maximum radiosensitization enhancement factor (REF) of 1.66 at 10% cell survival fraction (SF) for the radiation of X-ray of 105 kVp [22]. In contrast, the REFs are 1.48, 1.18, and 1.17 for the radiations of X-ray of 220 kVp, Cs-137 γ-ray (662 kVp), and X-ray of 6 MVp, respectively; i.e., the higher the photon energy, the lower the REF of GNPs [22]. This is because that the K-shell binding energy of electrons in gold is 80.7 keV. Additionally, Enferadi et al. used ultrasmall GNP-PEG (size: 2.6 nm) as radiosensitizer for different radiation sources: X-rays, Gamma ray of Cs-137 γ-ray and proton beam. Their results show that GNP-PEG provides a significant enhancement on all these radiotherapies [20]. As we know, GNPs are internalized via endocytosis, and then certain number of GNPs are aggregated and enclosed in thousands of vehicles within cytoplasm via organelle fusion [22, 27]. A few of studies used Monte Carlo simulation to investigate the mechanism of radiosensitization of GNPs on enhancing radiobiological efficacy [28–35]. In principle, the ionizing radiation can induce ejected electrons from GNPs through Auger effect, Compton effect, and photoelectric effect [36, 37]. The ejected electrons (photoelectrons, Auger electrons) and ionized electrons in water can produce excessive free radicals, particularly ROS [36]. Consequently, the excessive ROS cause the cellular damage, resulting in apoptosis and necrosis [38–46]. The relationship between the disruption of cytoskeleton and the excessive ROS induced in GNPs-uptake cells irradiated by a femtosecond laser (two-photon effect) has been verified [27]. This is to say that the damage on organelles by excessive ROS is another pathway to kill tumor cells, except the DSB of DNA.

In this paper, we quantitatively study the REF of non-targeted GNPs of 55-nm size on Cs-137 γ-ray radiotherapy from the curve of cell SF versus radiation dose [20, 22, 47]. We aim to provide more biological evidences to elucidate the mechanism of GNPs-enhanced ROS inducing the damage of organelles (mitochondria and cytoskeletons) to cause apoptosis or necrosis. Our results may pave a way to using GNPs as radiosensitizer to increase the production of ROS for raising the tumoricidal efficacy of radiotherapy, which might be useful to treat certain radioresistant tumor cells.

Method and Materials

We synthesized GNPs with an average size of 55 nm according to the previous synthesis recipe [27]. Additionally, the concentration of GNPs was measured by an inductively coupled plasma atomic emission spectroscopy (Agilent 5110) for experimental preparation. For our experiments, GNPs colloids of different concentrations were prepared. In our study, physics and biology experiments were conducted, individually. Two systems of Cs-137 γ-ray were used for radiation: MDS: Gammacell 40 Exactor (Canada) and Varian Medical Systems (UK). In fact, the radiation sources of Cs-137 are the same for both systems; the configuration of the Gammacell 40 Exactor facilitates the experiments of samples in tubes, and the configuration of Varian Medical Systems is for the experiments of cells on culture plates. The former was used for the experiments of inducing ROS in GNP colloid and the cell viability (clonogenic assay), and the latter was for the experiments of the damage of cellular organelles. For physics experiment, GNPs suspension (aqueous solution) was irradiated by Cs-137 (MDS: Gammacell 40 Exactor) for the measurement of ROS. An enzyme-linked immunosorbent assay (ELISA) reader (SpectraMax i3x, Molecular Devices, USA) was used to measure ROS with a labeling kit of Carboxy-H2DCFDA. In the presence of ROS, the DCFH of this kit can be converted to DCF, which is highly fluorescent as being excited by a light within the region of 488 nm to 495 nm.

For biology experiments, cell line of A431, human epidermoid carcinoma, was used for our experiment [27]. These cells were co-cultivated with a medium of 80-ppm GNPs for 24 h in advance of our experiments. Figure 1A shows the transmission electron microscope (TEM) image of cells with GNPs uptake, where the aggregation of GNPs enclosed by vesicles in cytoplasm is caused by the endocytosis and vesicle fusion [48]. The dark-field microscope (100×, ZEISS) image of cells with GNPs uptake is shown in Fig. 1C, where the bright spots in cytoplasm are due to the scattered light from these vesicles with certain number of GNPs. Figure 1B is the image of the controls without GNPs.

For the LSCM image, the nuclei of cells are stained by Hoechest 33,342, and the ROS labeling kit is Carboxy-H2DCFDA. Additionally, the kits for labeling mitochondria and cytoskeletons are MitoCapture™ and Alexa Fluor™ 488 Phalloidin, respectively. A laser scanning confocal microscopy (LSCM) (ZEISS LSM 780 META) is used to acquiring the cellular fluorescence images for detecting the labeling ROS or organelles. The excitation wavelength of laser and the emission passband of filter for exciting and detecting the fluorescence of different kits for the images of LSCM are listed in Additional file 1:

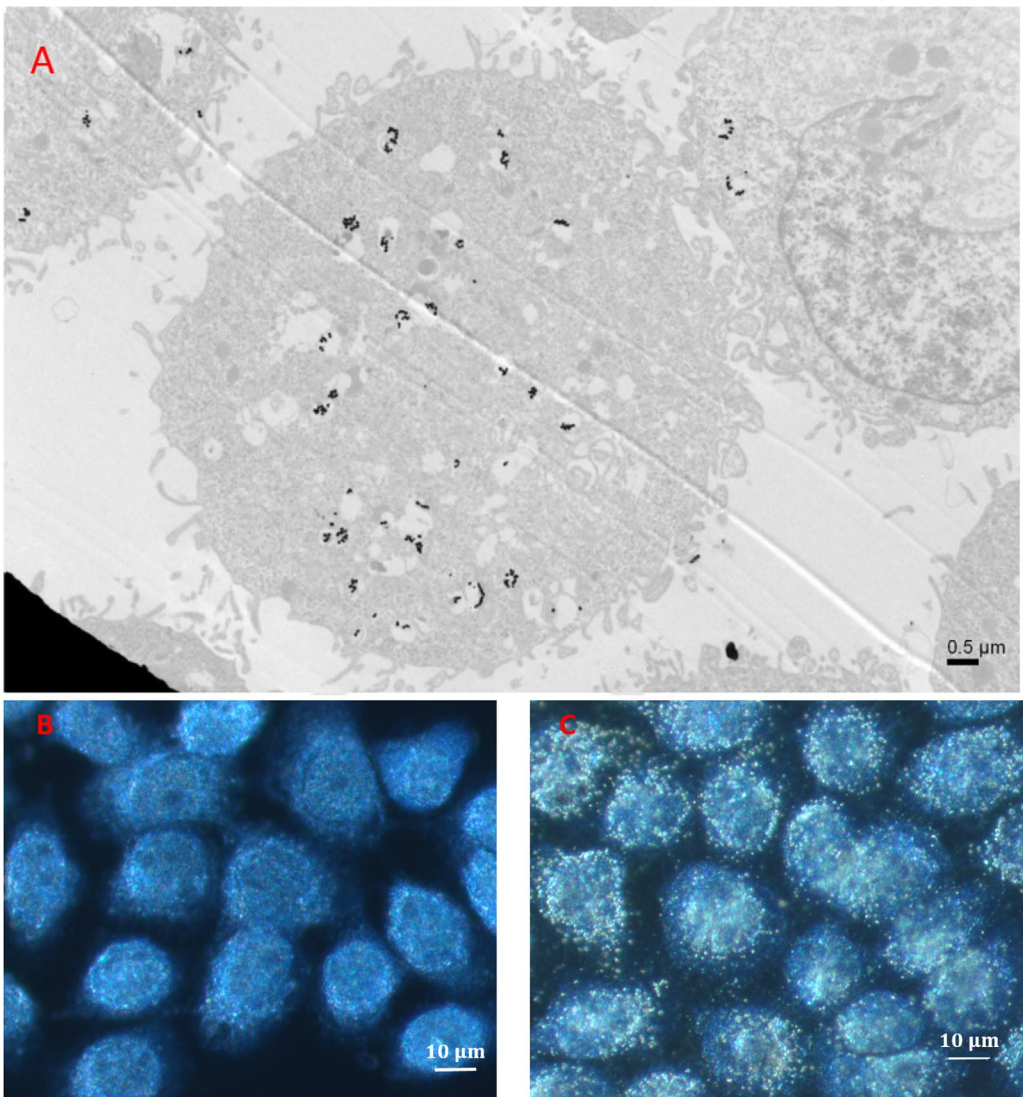

Fig. 1 **A** TEM image of GNPs-uptake cells. Black dots in the image are GNPs; certain number of GNPs are enclosed in vesicles through the endocytosis and fusion. **B** and **C** the dark-field microscope images of the controls and GNPs-uptake cells. Bright spots in **C** are the light scattering of these GNPs contained in vesicles. In contrast, there is no light scattering in controls

Table S1. Notice that the colors in the images of LSCM are the pseudocolors not the real ones of fluorescence.

Results and Discussion

First, the amounts of ROS produced in GNPs suspensions of different concentrations irradiated by 6 Gy Cs-137 were measured by ELISA reader, as plotted in **Fig. 2**. The linear regressions of the intensity of ROS kit (y) for dose 0 Gy and 6 Gy in terms of the concentration (x) of GNPs are $469x$-258.8 and $1076.8x$-384.8, respectively. The former can be regarded as the baseline. The slope of the line of 6 Gy is significantly larger than that of the control (0 Gy). These results demonstrate that the amount of produced ROS in aqueous solution of GNPs is increased as the concentration increases.

Biological Experiments

First, the cells of A431 were co-cultivated with a medium of 80-ppm GNPs for 24 h in advance. Subsequently, these GNPs-uptake cells were irradiated by Cs-137 with a dose of 6 Gy. Right after the irradiation, the fluorescence expression of kit (Carboxy-H2DCFDA) for labeling ROS in these cells measured by LSCM is shown in Fig. 3 (magnitude: ×63). The conditions of LSCM are listed in Additional file 1: Table S1. In addition, a low-magnitude (×20) image is shown in Additional file 1: Fig. S1. The

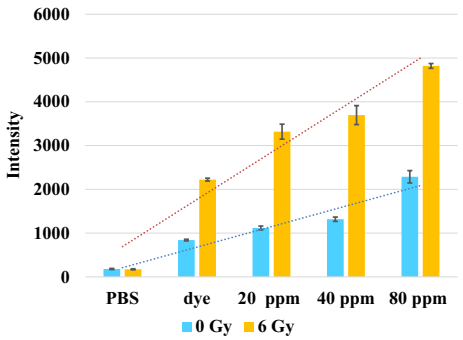

Fig. 2 Fluorescence expression of ROS kit in GNPs suspension versus various concentrations irradiated by 6 Gy Cs-137. Kit for ROS: Carboxy-H2DCFDA. Excitation wavelength: 495 nm, and emission wavelength: 529 nm for ELISA. Dash lines: linear regression

results demonstrate that after the irradiation, the amount of ROS in these GNPs-uptake cells is significantly higher than that in the control group, as shown in Fig. 3B and D. Although the lifetime of ROS is short, the induced damages of ROS (oxidative stress) on the organelles are long term.

Furthermore, we investigated the ROS-induced damages on cellular organelles (e.g., mitochondria and cytoskeletons) by using LSCM. In Fig. 4 (magnification: ×100), the bright spots in these cell images represent the fluorescence expression of active mitochondria (labeled by MitoCapture™) in cells, 48 h after the irradiation of 6 Gy Cs-137 (Varian Medical Systems). Obviously, the numbers of active mitochondria in the controls and the GNPs-uptake cells exposed to the radiation are significantly reduced, in comparison with these cells without

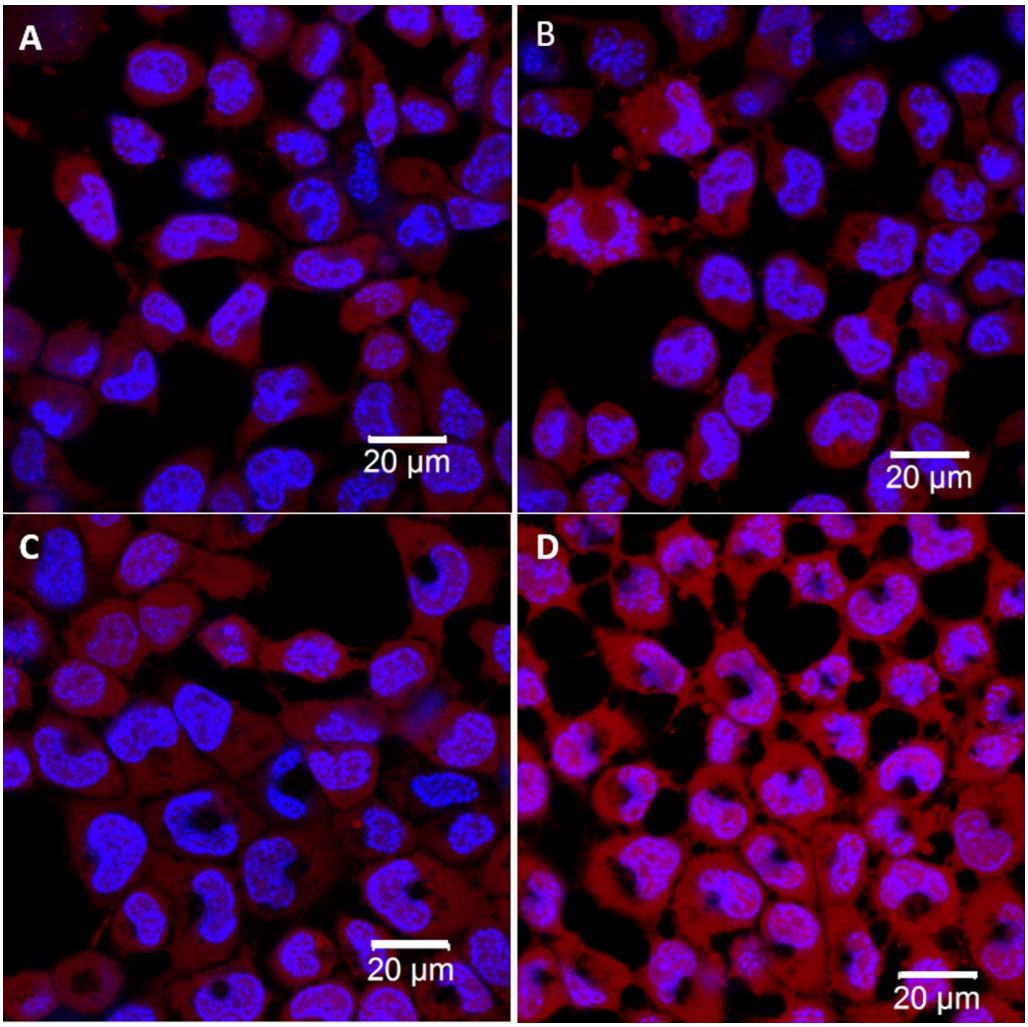

Fig. 3 Cell fluorescence images of LSCM for ROS kit irradiated by Cs-137 with a dose of 6 Gy (magnification: × 63). **A** and **B** are the images of the controls without and with irradiation of Cs-137, respectively. **C** and **D** the images of the GNPs-uptake cells without and with irradiation, respectively. Kit for ROS: Carboxy-H2DCFDA (red). Excitation laser: 488 nm; emission filter: 509–535 nm. Kit for nuclei: Hoechest 33,342 (blue)

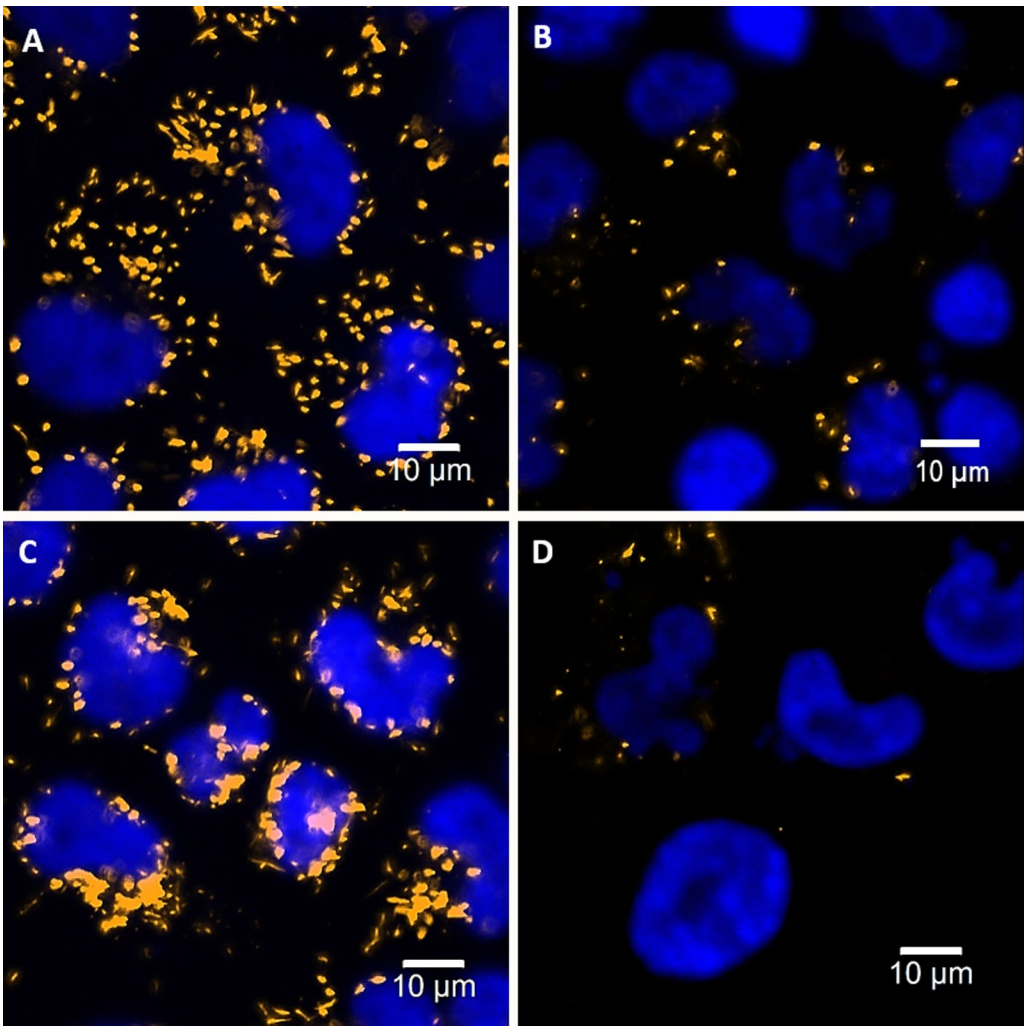

Fig. 4 Cell fluorescence images of LSCM for labeled activate mitochondria, 48 h after irradiation of 6 Gy Cs-137 (magnification: × 100). **A** and **B** are the images of the controls without and with irradiation of Cs-137, respectively. **C** and **D** are the images of the GNPs-uptake cells without and with irradiation, respectively. Kit for mitochondria: MitoCapture™ (yellow). Kit for nuclei: Hoechest 33,342 (blue)

irradiation. Moreover, the number of active mitochondria in these GNPs-uptake cells is obviously lower than that of the controls, as irradiated by Cs-137 (Fig. 4B and D). This is an evidence of the mitochondrial damage caused by the excessive ROS generated from GNPs in these cells, as irradiated by Cs-137. In addition, a low-magnitude (×20) image is shown in Additional file 1: Fig. S2. This phenomenon is due to that the excessive ROS could cause the dysregulation of mitochondria, including the damage of mitochondrial DNA [49].

We also investigated the ROS-induced damage on the cytoskeletons. Figure 5 (magnification: ×20) shows the fluorescence expression (green) of the cytoskeletons in cells, labeled by Alexa Fluor™ 488 Phalloidin. Before irradiation, the integrities of the cytoskeletons of the controls and the GNP-uptake cells are almost the same. However, the disruptions of cytoskeleton in these GNPs-uptake cells are more severe than those in the controls, 48 h after the irradiation of 6 Gy Cs-137 (Varian Medical Systems), in comparison with the control. This could be a consequence of cytoskeleton disruption caused by the excessive ROS, e.g., hydroxyl free radicals. The reason is that ROS can induce the depolymerization of actin filaments. As we know, cytoskeleton consists of actin filaments, intermediate filaments, and microtubules. The major function of cytoskeleton is to maintain the cell shape. Hence, once the integrity of cytoskeleton is broken by the excessive ROS, the cellular swelling is induced. A high-magnitude (×100) image is shown in Additional file 1: Fig. S3. Additionally, the

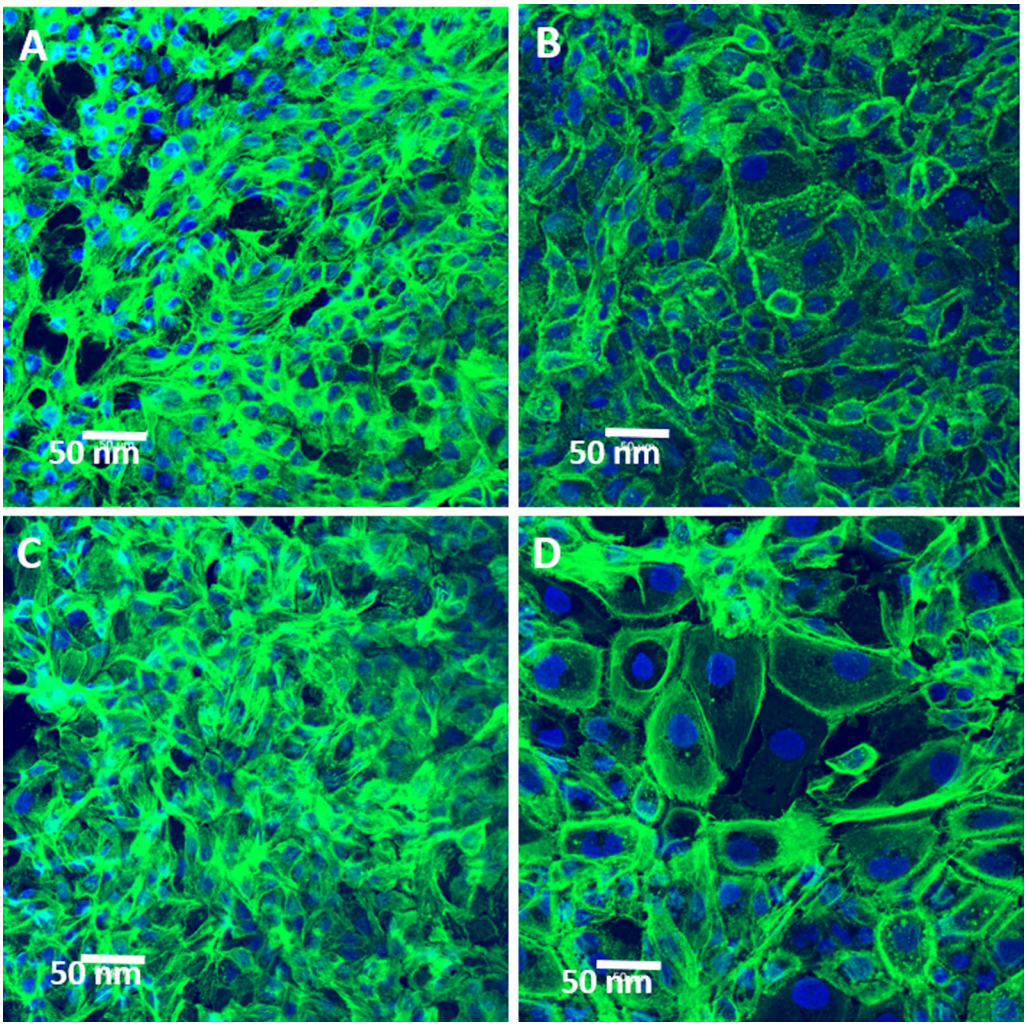

Fig. 5 Cell fluorescence images of LSCM for labeled cytoskeletons, 48 h after the irradiation of Cs-137 with a dose of 6 Gy (magnification: × 20). **A** and **B** are the images of the controls without and with irradiation of Cs-137, respectively. **C** and **D** the images of the GNPs-uptake cells without and with irradiation, respectively. Kit for cytoskeletons: Alexa Fluor™ 488 Phalloidin (green). Kit for nuclei: Hoechest 33,342 (blue)

morphology of a bigger nucleus could be due to the incomplete mitosis, which is an early indication of apoptosis caused by DNA damage.

Furthermore, we used the clonogenic assay method to measure the viability of A431 cells in vitro, 8 days after Cs-137 (MDS: Gammacell 40 Exactor) irradiation of different doses (0, 2, 4, 6 Gy). Using a fitting model of exponential decay in terms of a function of a linear and quadratic forms of dose, we obtain the estimated curves of the SFs of the GNPs-uptake cells and the control. Figure 6 shows the curves of SFs for the GNPs-uptake cells and the control (without GNPs co-cultivation) versus radiation dose. From the two curves, the amplification factor (AF) of GNP on cell SF at a specific dose is defined as the ratio of SF difference,

$$\mathrm{AF} = \frac{\mathrm{SF}_{\mathrm{control}} - \mathrm{SF}_{\mathrm{with\ GNPs}}}{\mathrm{SF}_{\mathrm{control}}} \times 100\% \quad (1)$$

The AFs at 2, 4 and 6 Gy are 13.6%, 28.2% and 36.1%, respectively. In addition, REF of GNPs on Cs-137 is defined as the ratio of the dose without GNPs to the dose with GNPs at a specific SF of 30%; REF is 1.292 [20, 22]. Not only AFs but also REF quantitatively illustrate that 55-nm GNPs are potential radiosensitizers for enhancing radiation therapy of Cs-137, as listed in Table 1.

In summary, our results show that ROS expressions in the 55-nm GNPs suspensions and in the GNPs-uptake cells irradiated by Cs-137 are significantly higher than those in the controls. Furthermore, the cell images of LSCM indicate the corresponding disruption

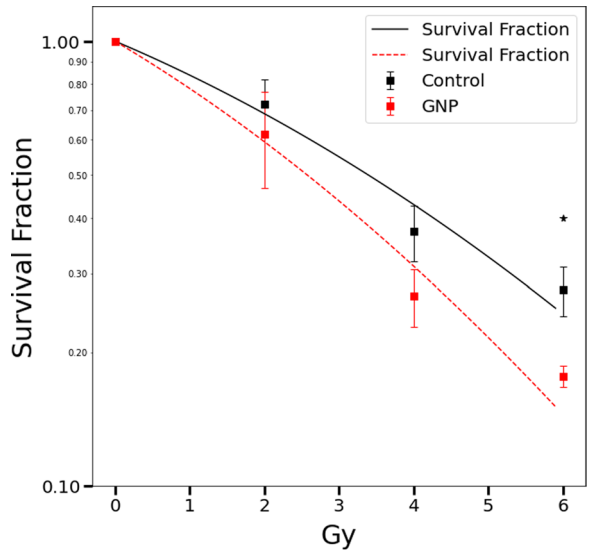

Fig. 6 Cell viability (in vitro clonogenic assay) of A431 with GNPs uptake; cell SF (8 days after Cs-137 irradiation) versus radiation dose. Control group: cells without GNPs co-culture. ★: $P < 0.02$

Table 1 AFs and REF of GNPs on Cs-137 therapy calculated from cell SF versus radiation dose

	AF (2 Gy)	AF (4 Gy)	AF (6 Gy)	REF at 30%
Cs-137 662 keV	13.60%	28.20%	36.13%	1.292

of cytoskeletons in these GNPs-uptake cells is more severe, compared to the control. In addition, the number of active mitochondria in these cells is dramatically reduced. The REF of GNPs on Cs-137 therapy at a SF of 30% is 1.29. The qualitative biological evidence and the quantitative REF prove the feasibility of using GNPs as radiosensitizer for Cs-137 radiotherapy.

Conclusion

In this paper, the efficacy of GNPs to increase the production of ROS under the irradiation of Cs-137 and the radiobiological effects on cells were studied. The cell images of LSCM verify the excessive expression of ROS produced in these cells with GNP uptake as being irradiated by Cs-137 radiation. Consequently, the significant disruption or damage of cytoskeletons and mitochondria, caused by the excessive ROS, in these cells were also observed by LSCM. Except the directional damage on DNA, the excessive ROS could cause the indirect damage on cellular organelles, e.g., mitochondria and cytoskeletons, to induce the apoptosis. According to the curves of cell SF versus radiation dose of Cs-137, the REF of GNPs is 1.29, which exhibits a significant enhancement on the tumoricidal efficacy of Cs-137 therapy. Our radiobiological results may pave a way to using GNPs as radiosensitizer to increase the production of ROS for raising tumoricidal efficacy of radiotherapy. This GNP-assisted radiotherapy might be particularly useful to treat certain radioresistant tumor cells. The In the future, the technique of surface modification, e.g., PEG, folic acid or peptide, on GNPs may be used to enhance the cellular uptake of GNPs for multi-functional medical applications of image, drug delivery, radiotherapy and so on [20, 22, 50–52].

Abbreviations

GNPs: Gold nanoparticles; ROS: Reactive oxygen species; LSCM: Laser scanning confocal microscopy; DSB: Double strand breaks; SF: Survival fraction; REF: Radiosensitization enhancement factor; AF: Amplification factor; ELISA: Enzyme-linked immunosorbent assay; TEM: Transmission electron microscope.

Supplementary Information

The online version contains supplementary material available at https://doi.org/10.1186/s11671-022-03761-w.

Additional file 1. **Table S1**: Parameters setup of the wavelengths of the excitation (Ex) lasers and the passbands of the emission (Em) filters of LSCM for inducing and detecting the fluorescence of different biomarkers (kits) for ROS and organelles in cells. **Fig. S1**: Cell fluorescence images of LSCM for labeled ROS irradiated by Cs-137 with a dose of 6 Gy (magnification: ×20); **Fig. S2**: Cell fluorescence images of LSCM for labeled activate mitochondria, 48 hours after irradiation of 6 Gy Cs-137 (magnification: ×20); Fig. S3: Cell fluorescence images of LSCM for labeled cytoskeletons, 48 hours after the irradiation of Cs-137 with a dose of 6 Gy (magnification: ×100).

Acknowledgements

The authors thank the Microscopy Center at Chang Gung University and Radiation Research Core Laboratory of Institute for Radiological Research, Chang Gung University/Chang Gung Memorial Hospital, Linkou for technical assistance.

Author Contributions

SWT, CHL and JWL drafted the manuscript. CHL, SYY, FHC, HCH and LKW conducted the experiments. JWL coordinated the projects and revised the manuscript. All authors read and approved the final manuscript.

Funding

The research was supported by Ministry of Science and Technology, Taiwan (MOST 109-2221-E-182-061, 110-2221-E-182-038-MY2) and Chang Gung Memorial Hospital (CIRPD2I0022, CIRPD2I0023).

Availability of Data and Materials

All the data and material are available in the manuscript.

Declarations

Competing interests

The authors declare no competing interests.

Author details

[1]Department of Biomedical Engineering, Chang Gung University, Taoyuan, Taiwan. [2]Department of Periodontics, Chang Gung Memorial Hospital, Taipei, Taiwan. [3]Department of Mechanical Engineering, Chang Gung University, Taoyuan, Taiwan. [4]Department of Medical Imaging and Radiological Sciences, Chang Gung University, Taoyuan, Taiwan. [5]Department of Radiation Oncology,

Chang Gung Memorial Hospital, Taoyuan, Taiwan. [6]Institute of Nuclear Engineering and Science, National Tsing Hua University, Hsinchu, Taiwan. [7]Proton and Radiation Therapy Center, Linkou Chang Gung Memorial Hospital, Taoyuan, Taiwan. [8]Radiation Biology Core Laboratory, Institute for Radiological Research, Chang Gung University/Chang Gung Memorial Hospital, Taoyuan, Taiwan. [9]Department of Mechanical Engineering, Ming Chi University of Technology, New Taipei City, Taiwan.

Received: 10 June 2022 Accepted: 1 December 2022
Published online: 14 December 2022

References

1. Azzam EI, Jay-Gerin JP, Pain D (2012) Ionizing radiation-induced metabolic oxidative stress and prolonged cell injury. Cancer Lett 327:48–60
2. Srinivasa US, Tana BWQ, Vellayappanb BA, Jeyasekharan AD (2019) ROS and the DNA damage response in cancer. Redox Biol 25:101084
3. Kam WWY, Banati RB (2013) Effects of ionizing radiation on mitochondria. Free Radic Biol Med 65:607–619
4. Pinar B, Henríquez-Hernández LA, Lara PC, Bordon E, Rodriguez-Gallego C, Lloret M, Nuñez MI, De Almodovar MR (2010) Radiation induced apoptosis and initial DNA damage are inversely related in locally advanced breast cancer patients. Radiat Oncol 5:85
5. Tremi I, Spyratou E, Souli M, Efstathopoulos EP, Makropoulou M, Georgakilas AG, Sihver L (2021) Requirements for designing an effective metallic nanoparticle (NP)-boosted radiation therapy (RT). Cancer 13:3185
6. Retif P, Pinel S, Toussaint M, Frochot C, Chouikrat R, Bastogne T, Barberi-Heyob M (2015) Nanoparticles for radiation therapy enhancement: the key parameters. Theranostics 5:1030–1045
7. McMahon SJ, Hyland WB, Muir MF, Coulter JA, Jain S, Butterworth KT, Schettino G, Dickson GR, Hounsell AR, O'Sullivan JM, Prise KM, Hirst DG, Currell FJ (2011) Biological consequences of nanoscale energy deposition near irradiated heavy atom nanoparticles. Sci Rep 1:18
8. Berbeco RI, Korideck H, Ngwa W, Kumar R, Patel J, Sridhar S, Johnson S, Price BD, Kimmelman A, Makrigiorgos GM (2012) DNA damage enhancement from gold nanoparticles for clinical MV photon beams. Radiat Res 178:604–608
9. McQuaid HN, Muir MF, Taggart LE, McMahon SJ, Coulter JA, Hyland WB, Jain S, Butterworth KT, Schettino G, Prise KM, Hirst DG, Botchway SW, Currell FJ (2016) Imaging and radiation effects of gold nanoparticles in tumour cells. Sci Rep 6:19442
10. Ghita M, McMahon SJ, Taggart LE, Butterworth KT, Schettino G, Prise KM (2017) A mechanistic study of gold nanoparticle radiosensitisation using targeted microbeam irradiation. Sci Rep 7:44752
11. Jain S, Hirst DG, O'Sullivan JM (2014) Gold nanoparticles as novel agents for cancer therapy. Br J Radiol 85:101–113
12. Jeremic B, Aguerri AR, Filipovic N (2013) Radiosensitization by gold nanoparticles. Clin Transl Oncol 15:593–601
13. Tsiamas P, Liu B, Cifter F, Ngwa WF, Berbeco RI, Kappas C, Theodorou K, Marcus K, Makrigiorgos MG, Sajo E, Zygmanski P (2013) Impact of beam quality on megavoltage radiotherapy treatment techniques utilizing gold nanoparticles for dose enhancement. Phys Med Biol 58:451
14. Jain S, Coulter JA, Hounsell AR, Butterworth KT, McMahon SJ (2011) Cell-specific radiosensitization by gold nanoparticles at megavoltage radiation energies. Int J Radiat Oncol Biol Phys 79:531–539
15. Wolfe T, Guidelli EJ, Gómez JA, Baffa O, Nicolucci P (2015) Experimental assessment of gold nanoparticle-mediated dose enhancement in radiation therapy beams using electron spin resonance dosimetry. Phys Med Biol 60:4465
16. Taggart LE, McMahon SJ, Currell FJ, Prise KM, Butterworth KT (2014) The role of mitochondrial function in gold nanoparticle mediated radiosensitisation. Cancer Nano 5:5
17. Kong T, Zeng J, Wang X, Yang X, Yang J, McQuarrie S, McEwan A, Roa W, Chen J, Xing JZ (2008) Enhancement of radiation cytotoxicity in breast-cancer cells by localized attachment of gold nanoparticles. Small 4:1537–1543
18. Chen N, Yang W, Bao Y, Xu H, Qin S, Tu Y (2015) BSA capped Au nanoparticle as an efficient sensitizer for glioblastoma tumor radiation therapy. RSC Adv 5:40514–40520
19. Antosh MP, Wijesinghe DD, Shrestha S, Lanou R, Huang YH, Hasselbacher T, Fox D, Neretti N, Sun S, Katenka N, Cooper LN, Andreev OA, Reshetnyak YK (2015) Enhancement of radiation effect on cancer cells by gold-pHLIP. PNAS 112:5372–5376
20. Enferadi M, Fu SY, Hong JH, Tung CJ, Chao TC, Wey SP, Chiu CH, Wang CC, Sadeghi M (2018) Radiosensitization of ultrasmall GNP-PEG-cRGDfK in ALTS1C1 exposed to therapeutic protons and kilovoltage and megavoltage photons. Int J Radiat Biol 94:124–136
21. Huo SD, Jin S, Ma X, Xue X, Yang K, Kumar A, Wang PC, Zhang J, Hu Z, Liang XJ (2014) Ultrasmall gold nanoparticles as carriers for nucleus-based gene therapy due to size-dependent nuclear entry. ACS Nano 8:5852–5862
22. Chithrani DB, Jelveh S, Jalali F, van Prooijen M, Allen C, Bristow RG, Hill RP, Jaffray DA (2010) Gold nanoparticles as radiation sensitizers in cancer therapy. Radiat Res 173:719–728
23. Tabatabaie F, Franich R, Feltis B, Geso M (2022) Oxidative damage to mitochondria enhanced by ionising radiation and gold nanoparticles in cancer cells. Int J Mol Sci 23:6887
24. Musielak M, Bo's-Liedke A, Piotrowski I, Kozak M, Suchorska W (2021) The role of gold nanorods in the response of prostate cancer and normal prostate cells to ionizing radiation—in vitro model. Int J Mol Sci 22:16
25. Huo SD, Ma HL, Huang KY, Liu J, Wei T, Jin SB, Zhang JC, He ST, Liang XJ (2013) Superior penetration and retention behavior of 50 nm gold nanoparticles in tumors. Cancer Res 73:319–330
26. Sah B, Antosh MP (2019) Effect of size on gold nanoparticles in radiation therapy: uptake and survival effects. J Nano Med 2:1013
27. Liaw JW, Kuo CY, Tsai SW (2021) The effect of quasi-spherical gold nanoparticles on two-photon induced reactive oxygen species for cell damage. Nanomaterials 11:1180
28. Leung MKK, Chow JCL, Chithrani BD, Lee MJG, Oms B, Jaffray DA (2011) Irradiation of gold nanoparticles by X-rays: Monte Carlo simulation of dose enhancements and the spatial properties of the secondary electrons production. Med Phys 38:624
29. Lin Y, McMahon SJ, Scarpelli M, Paganetti H, Schuemann J (2014) Comparing gold nano-particle enhanced radiotherapy with protons, megavoltage photons and kilovoltage photons: a Monte Carlo simulation. Phys Med Biol 59:7675
30. Xie WZ, Friedland W, Li WB, Li CY, Oeh U, Qiu R, Li JL, Hoeschen C (2015) Simulation on the molecular radiosensitization effect of gold nanoparticles in cells irradiated by X-rays. Phys Med Biol 60:6195
31. Lechtman E, Mashouf S, Chattopadhyay N, Keller BM, Lai P, Cai Z, Reilly RM, Pignol JP (2013) A Monte Carlo-based model of gold nanoparticle radiosensitization accounting for increased radiobiological effectiveness. Phys Med Biol 58:3075
32. Kirkby C, Ghasroddashti E (2015) Targeting mitochondria in cancer cells using gold nanoparticle-enhanced radiotherapy: a Monte Carlo study. Med Phys 42:1119–1128
33. Douglass M, Bezak E, Penfold S (2013) Monte Carlo investigation of the increased radiation deposition due to gold nanoparticles using kilovoltage and megavoltage photons in a 3D randomized cell model. Med Phys 40:071710
34. Lechtman E, Pignol JP (2017) Interplay between the gold nanoparticle sub-cellular localization, size, and the photon energy for radiosensitization. Sci Rep 7:13268
35. Hahn MB, Villate JMZ (2021) Combined cell and nanoparticle models for TOPAS to study radiation dose enhancement in cell organelles. Sci Rep 11:6721
36. Misawa M, Takahashi J (2011) Generation of reactive oxygen species induced by gold nanoparticles under X-ray and UV irradiations. Nanomedicine 7:604–614
37. Kuncic Z, Lacombe S (2018) Nanoparticle radio-enhancement: principles, progress and application to cancer treatment. Phys Med Biol 63:02TR01
38. Rosa S, Connolly C, Schettino G, Butterworth KT, Prise KM (2017) Biological mechanisms of gold nanoparticle radiosensitization. Cancer Nano 8:2
39. Hossain M, Su M (2012) Nanoparticle location and material-dependent dose enhancement in X-ray radiation therapy. J Phys Chem C 116:23047–23052
40. Cui L, Tse K, Zahedi P, Harding SM, Zafarana G, Jaffray DA, Bristow RG, Allen C (2014) Hypoxia and cellular localization influence the radiosensitizing effect of gold nanoparticles (AuNPs) in breast cancer cells. Radiat Res 182:475–488

41. Chen Y, Yang J, Fu S, Wu J (2020) Gold nanoparticles as radiosensitizers in cancer radiotherapy. Int J Nanomedicine 15:9407–9430
42. Jia S, Ge S, Fan X, Leong KW, Ruan J (2021) Promoting reactive oxygen species generation: a key strategy in nanosensitizer-mediated radiotherapy. Nanomedicine 16:759–778
43. Choi J, Jung KO, Graves EE, Pratx G (2018) A gold nanoparticle system for enhancement of radiotherapy and simultaneous monitoring of reactive-oxygen-species formation. Nanotechnology 29:504001
44. Roa W, Zhang X, Guo L, Shaw A, Hu X, Xiong Y, Gulavita S, Patel S, Sun X, Chen J, Moore R, Xing JZ (2009) Gold nanoparticle sensitize radiotherapy of prostate cancer cells by regulation of the cell cycle. Nanotechnology 20:375101
45. Butterworth KT, McMahon SJ, Taggart LE, Prise KM (2013) Radiosensitization by gold nanoparticles: effective at megavoltage energies and potential role of oxidative stress. Transl Cancer Res 2:269–279
46. Haume K, Rosa S, Grellet S, Śmiałek MA, Butterworth KT, Solov'yov AV, Prise KM, Golding J, Mason NJ (2016) Gold nanoparticles for cancer radiotherapy: a review. Cancer Nanotechnol 7:8
47. McMahon SJ, Hyland WB, Muir MF, Coulter JA, Jain S, Butterworth KT, Schettino G, Dickson GR, Hounsell AR, O'Sullivan JM, Prise KM, Hirst DG, Currell FJ (2011) Nanodosimetric effects of gold nanoparticles in megavoltage radiation therapy. Radiother Oncol 100:412–416
48. Tsai SW, Chen YY, Liaw JW (2008) Compound cellular imaging of laser scanning confocal microscopy by using gold nanoparticles and dyes. Sensors 8:2306–2316
49. Houten BV, Woshner V, Santos JH (2006) Role of mitochondrial DNA in toxic responses to oxidative stress. DNA Repair 5:145–152
50. Tsai SW, Liaw JW, Hsu FY, Chen YY, Yeh MH, Lyu MJ (2008) Surface-modified gold nanoparticles with folic acid as optical probes for cellular imaging. Sensors 8:6660–6673
51. Al-Dulimi AG, Al-Saffar AZ, Sulaiman GM, Khalil KAA, Khashan KS, Al-Shmgani HSA, Ahmed EM (2020) Immobilization of L-asparaginase on gold nanoparticles for novel drug delivery approach as anti-cancer agent against human breast carcinoma cells. J Mater Res Technol 9(6):15394–15411
52. Al-Omar MS, Jabir M, Karsh E, Kadhim R, Sulaiman GM, Taqi ZJ, Khashan KS, Mohammed HA, Khan RA, Mohammed SAA (2021) Gold nanoparticles and graphene oxide flakes enhance cancer cells' phagocytosis through granzyme-perforin-dependent biomechanism. Nanomaterials 11:1382

Publisher's Note